Estimating the minimum ignition energy of spark-ignited fuel/air mixtures: preliminary steps towards a novel modelling approach

Journal of Physics: Conference Series **2893** (2024) 012093 doi:10.1088/1742-6596/2893/1/012093

Estimating the minimum ignition energy of spark-ignited fuel/air mixtures: preliminary steps towards a novel modelling approach

Marco Pretto, Enrico De Betta, Pietro Giannattasio

Dipartimento Politecnico di Ingegneria e Architettura, Università degli Studi di Udine, Via delle Scienze 206, 33100, Udine, Italy

e-mail addresses: marco.pretto@uniud.it; debetta.enrico@spes.uniud.it; pietro.giannattasio@uniud.it;

Abstract. In spark-ignition (SI) engines, the achievement of a fast combustion with low cycle-to-cycle variation is highly dependent on the successful initiation of a flame kernel from the spark plug. Its growth can be sped up by increasing the electrical energy supply, but at the cost of higher plug wear, whereas too little energy may result in an ignition failure. Therefore, knowledge of the minimum ignition energy (MIE) of a fuel/air mixture is of key importance to guarantee a proper combustion process at minimal cost. To model the MIE several approaches have been proposed in literature, primarily derived from the experiments conducted by Lewis and Von Elbe and their resulting theory of quenching distances. However, these approaches appear in conflict with more recent experimental outcomes, and the impact of the ignition device is neglected. This work proposes a novel approach for modelling the MIE, which is based on a flame kernel expansion model recently proposed in another paper. In this approach, the proposed model, which has general validity, is specialized to the particular case of the estimation of the MIE, supplied via an electrical breakdown. A model advancement is also included that consists in the quantification, albeit at a preliminary level, of the impact of different gap distances and spark plug quenching effects on the flame kernel development. The results are validated against literature models and experimental data for two fuels, propane and hydrogen, and multiple equivalence ratios. In contrast with the noticeable MIE overestimation of literature models, for propane the proposed approach leads to better results compared to the experiments. Instead, for hydrogen a tendency towards a MIE underestimation is observed, especially for lean mixtures. The model is also tested for SI-engine-relevant conditions, showing satisfactory overall trends. The key source of error seems related to the very complex kernel-electrode interaction, the modelling of which will be improved in future developments.

1. Introduction

The minimum ignition energy (MIE), defined as the minimal energy required to initiate combustion in a flammable mixture under specified pressure and temperature conditions, holds significant importance. It is a pivotal factor in enhancing combustion stability and fuel efficiency within spark-ignited (SI) internal combustion engines (ICEs), while concurrently mitigating the risks associated with unintended explosions in industrial and aviation sectors. An extensive series of experiments aimed at determining the MIE for various fuels was conducted by Lewis and Von Elbe [1]. These experiments involved measuring the energy stored in a capacitor at a known voltage, which was then discharged through the electrodes of a spark plug. With a similar approach, Moorhouse et al. [2]

determined the MIE for some hydrocarbon/air mixtures using an ignition probability criterion of 0.8, which means that there is a probability of 80% that a specific electrical energy input will cause the ignition of a flammable mixture. In their study, the MIE values for propane/air mixtures were found to be more than double than those reported by Lewis and Von Elbe [1]. Instead, Randeberg et al. [3] conducted experiments on dust clouds and propane, obtaining one-order-of-magnitude lower MIE values compared to Lewis and Von Elbe [1]. The discrepancies observed in these contributions are probably the consequence of different experimental set-ups (e.g., shorter spark duration), but another key reason of such different results derives from the fact that the ignition phenomenon is a stochastic event. Indeed, statistical analyses have been performed [4] [5] [6] to correlate the probability of a successful ignition with the spark energy, further confirming this stochastic behaviour. Such randomness, which in the end affects the entire combustion development, makes it hard to match accurately the experimental data using any prediction model.

In addition to the sheer problem of predicting the MIE, modelling the ignition of a combustible mixture, whether successful or unsuccessful, presents considerable obstacles in itself. Elements such as electrical breakdown, interaction between flame kernel and electrodes, dynamics of burned gases, and combustion kinetics at non-adiabatic flame temperatures must all be taken into account. Although Computational Fluid Dynamics (CFD) coupled with reaction mechanisms offers a powerful tool for studying the ignition, and hence the MIE [7] [8], it is undeniable that this approach is very time-consuming and rather impractical for the simulation of ICE combustion.

In this framework, the present contribution aims to provide a novel approach for the MIE estimation of fuel/air mixtures, which is based on the simulation of the expansion of a flame kernel at very low ignition energies. This is done using a novel kernel expansion model proposed by the present authors and based on the thermodiffusive theory [9]. It is worth noting that the thermodiffusive theory assumes constant density and no convective flows [10], and therefore the simulation of an actual flame kernel requires appropriate adjustments of the theory, which were partially carried out [9]. In addition, this theory assumes a perfectly spherical kernel geometry, but this is inconsistent with the presence of the spark plug electrodes. Therefore, appropriate modelling changes are necessary, and this work illustrates some preliminary strategies to consider these elements.

In this paper, Section 2 briefly illustrates the main analytical models for the MIE determination, and then presents the authors' flame kernel expansion model together with the preliminary strategies to account for the effect of actual ignition devices (e.g. spark plugs) on the kernel development. In Section 3, the validation of the proposed approach is conducted and results for typical ICE conditions are shown. Finally, conclusions and future developments are presented in Section 4.

2. Methodology

2.1. Analytical MIE estimation models from literature

In general, all analytical models for estimating the MIE are independent of the ignition device, and they are based on finding the smallest spherical kernel able to expand successfully, often denoted as the critical flame kernel. Lewis and Von Elbe [1] introduced two relations to estimate the MIE, represented by equations (1) and (2). In equation (1), the MIE corresponds to the energy required to balance the heat lost from the surface of the kernel, which has adiabatic flame temperature T_{ad} and diameter equal to the quenching distance, d_q, towards the fresh mixture at temperature T_u. In equation (2), the MIE corresponds to the energy required to heat up a sphere of diameter d_q from T_u to T_{ad}:

$$MIE = \pi d_q^2 \frac{\bar{\lambda}(T_{ad} - T_u)}{S_L^0}, \tag{1}$$

$$MIE = \frac{1}{6}\pi d_q^3 \rho_{ad} \bar{c_p}(T_{ad} - T_u), \tag{2}$$

where S_L^0 is the planar adiabatic laminar flame speed, ρ_{ad} is the burned gas density, $\bar{\lambda}$ and $\bar{c_p}$ are the thermal conductivity and specific heat at constant pressure averaged between burned and fresh

mixture. Both of these models are able to capture the overall MIE behaviour, but challenging is the quantification of d_q, for which analytical calculations require so many simplifications that only rough estimates, such as the $d_q = \sqrt{6}\delta_L$ given by Turns [11], δ_L being the laminar flame thickness, can be achieved. As a result, while equations (1) and (2) continue to enjoy ample use even today [12] [13], d_q needs to be calibrated on a case-by-case basis, usually relying on experimental data.

A second key limitation of these models is that mass diffusion is neglected, especially in terms of the Lewis number, Le, which is the ratio between heat and mass diffusion. However, as demonstrated by He [14], Le is the parameter most affecting the flame stretch, which dominates the entire kernel response. Firstly, flame stretch changes the critical radius to be exceeded by the kernel to achieve successful ignition, which explains why calibration of d_q is required. Secondly, flame stretch is very often correlated linearly with the kernel expansion speed, but experimental evidence shows that for small (under 6-8 mm) kernels this relationship is highly non-linear [15]. Additionally, flame stretch plays a significant role in modifying the kernel temperature, T_f, when $Le \neq 1$, resulting in $T_f \neq T_{ad}$ [16] [17]. All these observations suggest that a kernel expansion model capable of capturing these effects could improve the MIE estimation.

2.2. Summary of the novel flame kernel expansion model

Recently, the authors of the present work introduced a model to describe the initiation and expansion of a spark-ignited flame kernel [9], which is summarized in this section. Concerning the ignition phase, it is assumed to occur via an electrical breakdown between two electrodes, which causes the formation of a plasma column that expands via a cylindrical shock wave, increasing its mass. The initial conditions for the expansion model, named $[\cdot]_i$, are set at the end of the breakdown, and their modelling, inspired by the work of Meyer and Wimmer [18], is further discussed in another paper [19]. Equations (3) yield the parameters for the end-of-breakdown column, including its radius $r_{i,cyl}$, absolute enthalpy h_i, and the time t_i required for pressure equalization after the shock wave:

$$\begin{cases} r_{i,cyl} = 0.5 r_c = 0.5 \left(\dfrac{E_{bd}}{3.94 \pi d_g p_u} \right)^{1/2}, \\ t_i = 1.5 t_c = 1.5 \left(\dfrac{r_c}{\sqrt{\gamma_u p_u / \rho_u}} \right), \\ (h_i - h_u) \rho_i V_i = \eta_{bd} E_{bd}, \qquad with\ V_i = \pi r_{i,cyl}^2 d_g. \end{cases} \tag{3}$$

In equations (3) r_c and t_c are characteristic time and length scales, E_{bd} is the breakdown energy deposited across spark gap d_g with efficiency η_{bd}, p_u is the uniform pressure at the end of expansion, γ_u is the heat capacity ratio of the fresh mixture, ρ_u its density, h_u its enthalpy, and V_i is the plasma volume. However, the kernel is assumed to expand spherically, and hence the initial radius is reported to that of the equivalent-volume sphere and computed as $r_i = (3V_i/4\pi)^{1/3}$. Initial temperature T_i is estimated from the absolute enthalpy h_i, since p_u is known and chemical equilibrium is assumed.

With the initial conditions set, the flame kernel expansion model is based on the solutions of 1D spherical mass, species, and energy conservation equations of the kernel [9], and it is supported by elements of the theoretical work of Yu and Chen on transient thermodiffusion [20], In this model, one-step combustion is assumed, which is controlled by the deficient reactant having mass fraction Y_A, while the pressure is constant and uniform. The flame front is assumed to be a zero-width reactive surface, while the pre-heat and mass diffusion zones extend into the unburned mixture. An illustration of the model along with temperature and deficient reactant profiles is shown in Figure 1.

A summary of the model is provided in this section. Starting from the conservation laws, a rearrangement of the equations is carried out [9] that leads to a two-equation system, which is reported in equations (4a) and (4b). Hereafter, quantities related to the fresh mixture at flame temperature are denoted as $[\cdot]_{u,f} = [\cdot]_u(T_f)$, while quantities concerning the burned gas as $[\cdot]_f$.

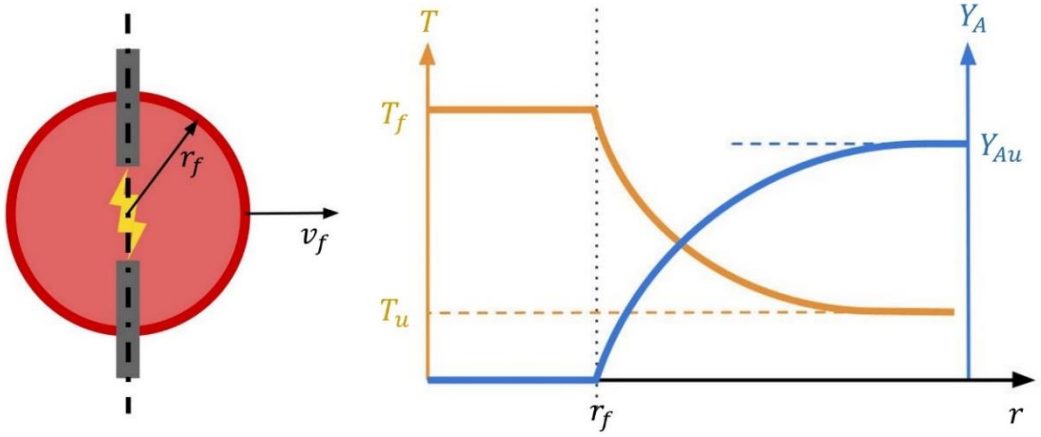

Figure 1 – Sketch of the flame kernel (left) and profiles of temperature and deficient reactant (right).

$$\begin{cases} m_f c_{p,f} \dfrac{dT_f}{dt} = A_f\left(\rho_u S_L^0 \omega_f + \dot{m}_{en}\right)(h_{u,f} - h_f) + A_f k_{u,f} C_T \left.\dfrac{\partial T}{\partial r}\right|_{r_f} + P_e, & \text{(4a)} \\ \dfrac{1}{Le}\left(\dfrac{k}{c_p}\right)_{u,f} \cdot C_A \left.\dfrac{\partial Y_A}{\partial r}\right|_{r_f} = Y_{Au}\rho_u S_L^0 \omega_f, & \text{(4b)} \end{cases}$$

where $\omega_f = \left(T_f/T_{ad}\right)^2 exp\left[-T_a/2\left(1/T_f - 1/T_{ad}\right)\right]$ expresses the dependency of the reaction rate on kernel temperature T_f, P_e is the arc/glow electric power and $\dot{m}_{en}$ is an entrainment mass flow, assumed proportional to P_e and taking into account non-spherical effects caused by this energy supply [21]. The system unknowns are kernel temperature T_f and radius r_f, being $v_f = dr_f/dt$ and $m_f = 4\pi\rho_f r_f^3/3$. However, these equations require the temperature and deficient reactant gradients at r_f, for which the results of transient thermodiffusive theory are used [20]. These gradients are:

$$\begin{cases} \left.\dfrac{\partial T}{\partial r}\right|_{r_f} = \left.\dfrac{\partial \theta}{\partial \varphi}\right|_R \dfrac{(T_{ad} - T_u)}{l_T^0} = -\dfrac{f_{uT}}{R}\left[\theta_f + \theta_i(\vartheta(x) - 1)\right]\dfrac{(T_{ad} - T_u)}{l_T^0}, \quad x = exp\left(-\dfrac{\pi^2 {f_{uT}}^2}{R^2}\tau\right), & \text{(5a)} \\ \left.\dfrac{\partial Y_A}{\partial r}\right|_{r_f} = \left.\dfrac{\partial y_A}{\partial \varphi}\right|_R \dfrac{Y_{Au}}{l_T^0} = \left.\dfrac{\partial y_A}{\partial \varphi}\right|_R = \dfrac{f_{uy}}{R}\vartheta(x)\dfrac{Y_{Au}}{l_T^0}, \quad x = exp\left(-\dfrac{\pi^2 {f_{uy}}^2}{LeR^2}\tau\right). & \text{(5b)} \end{cases}$$

The required non-dimensional terms are defined in equations (6) using the planar adiabatic flame, and especially its expansion speed $v_L^0 = S_L^0 \cdot \rho_u/\rho_{ad}$, as the reference condition. This accounts for the convective flows due to thermal expansion, unlike thermodiffusion, which assumes constant density.

$$\begin{aligned} l_T^0 &= \frac{k_{ad}}{\rho_{ad} c_{p,ad} v_L^0}, \quad t_L^0 = \frac{l_T^0}{v_L^0}, \quad R = \frac{r_f}{l_T^0}, \quad \tau = \frac{t}{t_L^0}, \quad U = \frac{dR}{d\tau} = \frac{v_f}{v_L^0}, \\ \theta &= \frac{T - T_u}{T_{ad} - T_u}, \quad y_A = \frac{Y_A}{Y_{Au}}, \quad Le = \frac{\alpha}{D_A}, \quad \varphi = \frac{r}{l_T^0}, \quad \sigma = \frac{r}{r_f} = \frac{\varphi}{R}. \end{aligned} \tag{6}$$

Then, equations (5a) and (5b) are completed by the Jacobi theta function, defined as $\vartheta(x) = 1 + 2\sum_{n=1}^{+\infty} x^{n^2}$, and by the terms f_{uT} and f_{uy}, computed according to the expressions below:

$$\begin{cases} f_{uT} = \dfrac{1}{\int_1^{+\infty} F_{uT} d\sigma}, & with\ F_{uT} = \dfrac{1}{\sigma^2} exp\left(-\dfrac{RU}{2}(\sigma^2 - 1)\right), \\ f_{uy} = \dfrac{1}{\int_1^{+\infty} F_{uy} d\sigma}, & with\ F_{uy} = \dfrac{1}{\sigma^2} exp\left(-\dfrac{RULe}{2}(\sigma^2 - 1)\right). \end{cases} \tag{7}$$

Finally, in equations (4a) and (4b) adjustment coefficients C_A and C_T are necessary to account for the variation of thermodynamic properties with temperature and mixture composition, also not covered by thermodiffusion. These coefficients can be computed exactly only under two extreme conditions, the adiabatic planar flame and the stationary flame ball, and their values are reported in Table 1. In all other cases, the coefficients will assume intermediate values.

Table 1 – Adjustment coefficients C_A and C_T for the adiabatic planar flame and the flame ball.

	Adiabatic planar flame $[\cdot]_{,ad}$	**Flame ball** $[\cdot]_{,z}$
$\boldsymbol{C_A}$	$\left(k/c_p\right)_{ad}/\left(k/c_p\right)_{u,ad}$	1
$\boldsymbol{C_T}$	$\frac{(h_{u,ad}-h_{ad})}{c_{p,ad}(T_{ad}-T_u)}\cdot\frac{k_{ad}}{k_{u,ad}}$	$\frac{h_{u,z}-h_z}{c_{p,u,z}(T_{ad}-T_u)}$

2.3. MIE estimation using the proposed kernel expansion model

The present expansion model enables predicting the flame kernel development under flame stretch of any intensity, thanks to the explicit consideration of the species conservation law and to the separation between pre-heat and mass diffusion zones, which in fact leads to two different gradients. This allows the model to predict even a stretch-induced kernel extinction, as done by the present authors for propane/air flames [9]. The two key model parameters are S_L^0, higher values of which promote the expansion, and Le, whose growth above 1 renders the expansion increasingly difficult, while T_a has a more modest effect. Given its capabilities, it is possible to apply this model for estimating the MIE of any fuel/air mixtures, and this can be done by finding the minimum energy at which a given kernel survives without extinguishing due to flame stretch. However, before doing so some modifications to the expansion model itself are required. Firstly, as highlighted in the literature [3], in MIE experiments the electrical energy from capacitive sparks is transferred to the gas almost entirely during and immediately after the breakdown, and arc/glow sparks can be neglected. Consequently, here it is assumed that the ignition energy is provided only during the breakdown phase, and hence $P_e = \dot{m}_{en} = 0$. This assumption is particularly valid for lower MIEs, because the energy stored in the capacitor is transferred very quickly. At the same time, P_e accounts also for the heat lost to the electrodes through a deposition efficiency, and this effect must be considered even when there is no external energy provided. To do so, a heat transfer rate, Q_w, is introduced in equation (4a) to replace P_e:

$$Q_w = -hA_w\left(T_f - T_u\right), \tag{8}$$

where h is the heat transfer coefficient and A_w is the contact area between the hot kernel expanding from the center of the spark gap and the electrodes, assumed to be at the temperature of the fresh mixture. The heat transfer always cools the flame kernel fostering its extinction, but it does so with increasing intensity as the gap gets smaller, since the kernel comes earlier into contact with the electrodes. Hence, small gap distances d_g are expected to require more energy to ignite the mixture compared to larger gaps. However, multiple experiments [1] [22] show that the MIE actually increases as d_g exceeds an optimum value. This is mainly because for long gaps the kernel starts as an elongated cylinder, which undergoes transition to a sphere during its expansion until it reaches a reasonable size, but also because longer gaps require higher breakdown voltage, which ultimately leads to higher E_{bd} [1]. Modelling these two phenomena is an extremely complicated task, which is why simplifications are made in this work. Firstly, E_{bd} is assumed to be supplied independently of the electric circuit, thus treating it as a freely chosen parameter. Then, concerning the cylinder-to-sphere transition, the kernel is assumed to remain spherical throughout the simulation, but a preliminary solution was implemented that attempts to account for this occurrence by modifying the normalized radius, $R = r_f/l_T^0$. The key idea is keeping the kernel as a sphere of radius r_f, but using a smaller effective radius $r_{f,eff}$ to compute R, which controls the gradients in equations (5) in such a way that a smaller R yields a stronger flame stretch. This reduction is assumed to subside when r_f reaches $d_g/2$, after which the

kernel is considered spherical and $r_{f,eff} = r_f$. In this work a cubic interpolation between $d_g/2$ and the end-of-breakdown cylinder radius, $r_{i,cyl}$, was chosen, which is expressed by equation (9):

$$r_{f,eff} = r_{i,cyl} - \frac{\left(r_f - r_{i,cyl}\right)^3}{\left(d_g/2 - r_{i,cyl}\right)^2} + 2\frac{\left(r_f - r_{i,cyl}\right)^2}{d_g/2 - r_{i,cyl}}. \quad (9)$$

An advantage of this expression is that $r_{f,eff}$, considered only for the computation of R, is continuous also in its derivative with respect to r_f at $d_g/2$. A visualization of $r_{f,eff}$ during the cylinder-to-sphere transition and its behaviour as described by equation (9) are shown in Figure 2.

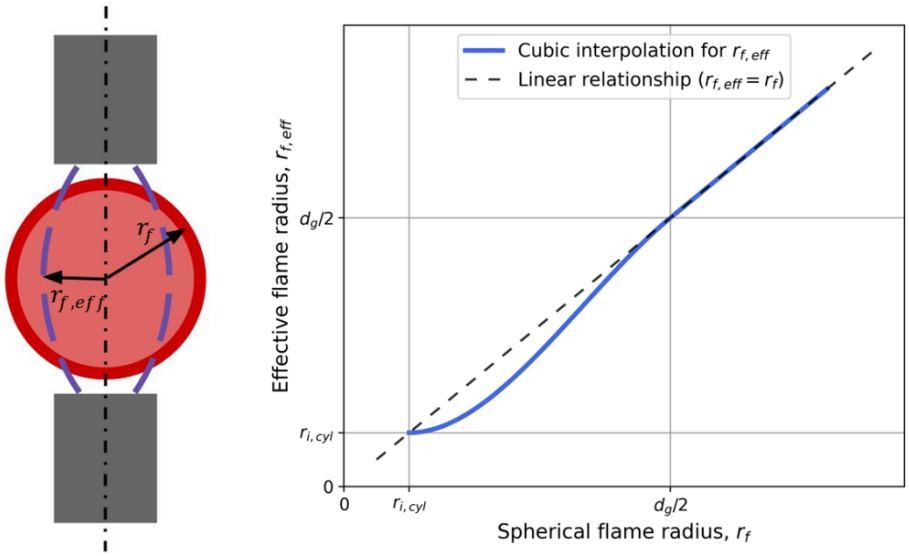

Figure 2 – Effective kernel radius $r_{f,eff}$ visualized (left) and estimated as per equation (9) (right).

Another issue in evaluating the MIE arises when the breakdown event is very intense, which leads to the formation of a toroidal structure that activates a large volume of gas around the electrodes. This occurrence has been observed experimentally [23] and numerically [24] [25], but this effect cannot be accounted for by the present analytical model, because an overall 1D spherical geometry is assumed, with amendments only for the aforementioned cylinder-to-sphere transition.

Having accounted for the heat losses to the electrodes and the altered kernel geometry, the MIE of a given spark-ignited fuel/air mixture can be estimated with a series of simulations in which the breakdown energy, E_{bd}, is steadily reduced from a high initial value until the kernel stops expanding and extinguishes due to flame stretch. The smallest E_{bd} that ensures successful self-sustained kernel propagation is selected as the MIE, while deposition efficiency $\eta_{bd} = 0.9$ is set as an average value following the literature [18]. For the extinction criterion, the first option would be to define it as the condition at which $U = v_f = 0$, but experiments [17] [26] show that actual kernels extinguish before $U = 0$. This is because at low v_f the flame front cannot entrain the reactants quickly enough to sustain the combustion, thus causing the kernel extinction, but the front still advances some more by stretching the reactive surface, for which the zero-width assumption made in this model is no longer valid. Following these observations, in this work the expansion speed threshold was set to $U = 0.1$, meaning that the kernel is considered extinguished if v_f drops below 10% of v_L^0. Finally, the statistical dispersion of the ignition phenomenon is neglected, as it goes beyond the scope of this model.

3. Results and discussion

In this section quantitative results on the MIE are presented and discussed for both the analytical models described in the literature and for the novel approach proposed in this work, with comparisons

to experimental results where possible. In accordance with Section 2, the present calculations require three key quantities: the planar adiabatic laminar flame speed, S_L^0, the activation temperature, T_a, and the mixture Lewis number, Le. These values were computed for each unburned mixture by following well-known literature methods based on the simulation of planar adiabatic flames, carried out using the software package Cantera [27]. In particular, after simulating the reference planar adiabatic flame from which to extract S_L^0, the adiabatic flame temperature was varied by slightly modifying the nitrogen content in the mixture, which enabled determination of T_a by computing the derivative of the mass flow with respect to T_{ad} [16]. Then, Le was computed as a weighted average of the Lewis numbers of excess and deficient reactants, with an equivalence-ratio-based weighting that makes use of T_a, taken as the value estimated in the previous step [28] [29].

Furthermore, for the present expansion model it is crucial to supply the two adjustment coefficients C_A and C_T, which are estimated with the expressions successfully tested for propane/air mixtures [9]. Their values are provided below as a function of U and with $j = (T, A)$:

$$C_j = \begin{cases} C_{j,ad} & if\ U > U_{max} = 0.5, \\ C_{j,z} + (C_{j,ad} - C_{j,z}) \cdot \dfrac{U - U_{min}}{U_{max} - U_{min}} & if\ U \in [U_{min};\ U_{max}], \\ C_{j,z} & if\ U < U_{min} = 0.2. \end{cases} \quad (10)$$

It is assumed that the planar adiabatic coefficients are most appropriate at higher expansion speeds, while the stationary flame ball ones at lower speeds, with a linear interpolation in between.

Finally, regarding the electrode configuration, for all simulations cylindrical electrodes with a diameter of 1.6 mm were considered, similar to the ones used by Lewis and Von Elbe [1]. It is evident that modifying their shape and size would impact the MIE results, since the contact area between flame kernel and electrodes depends on this parameter.

3.1. Behaviour of the MIE prediction model for different gap sizes and heat transfer intensities

The expansion model requires no calibration parameters other than C_A and C_T, computed with equation (10). However, some electrode-related quantities remain uncertain, such as the heat transfer coefficient. Therefore, several simulations were first conducted to verify the sensitivity of the MIE to variations in this parameter as the gap distance changes. A propane/air mixture at atmospheric conditions and $\phi = 1.3$, as used by Wähner et al. [6], was chosen for the calculations.

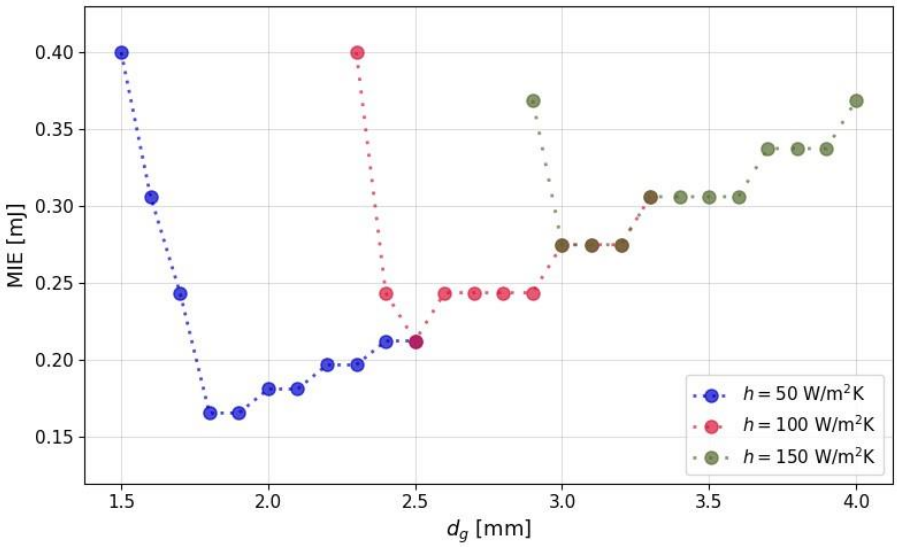

Figure 3 – MIE as a function of gap size d_g using different values of heat transfer coefficient h.

Figure 3 illustrates the MIE as a function of gap distance d_g for three different values of the heat transfer coefficient ($h = 50, 100$, and 150 W/m^{2}K). The electrodes effectively cool the flame kernel when d_g is small, resulting in a rapid decrease in the MIE as d_g increases. However, as d_g becomes larger the MIE starts increasing, and this is caused by the effective flame radius correction in equation (9): as d_g rises, this correction becomes progressively more significant, because $r_{f,eff}$ remains smaller than r_f for longer. This increases the flame front gradients, equations (5a,b), and ultimately results in a more intense kernel heat loss towards the unburned mixture, which is counteracted only by a higher spark energy. Therefore, by virtue of these two opposite flame kernel responses at small and large d_g, it is always possible to identify an optimal d_g for which the MIE is lowest.

Figure 3 qualitatively reproduces the trends reported in the literature [1] [6], and the energy values largely agree with the experimental ones for cases with $h = 100$ and 150 W/m^{2}K. However, in these cases the optimal d_g values are larger than those in the literature [6], which range from 1.7 to 1.9 mm and are closer to those predicted with $h = 50$ W/m^{2}K. These discrepancies may be attributed to different electrode shapes and energy supply methods, unclear in the experiments but involving only the breakdown energy in this work, but also to a too simplified modelling of the phenomena mentioned in Section 2.3. Finally, some MIE overlap with different h can be observed, which is caused mainly by the fact that changing h alters the balance between electrode heat losses and geometrical transition, leading the MIE minima at higher h to overlap the large-gap MIEs at lower h. In light of these results, $h = 100$ W/m^{2}K was assumed for all the following simulations, and gap distance d_g was taken as that yielding the smallest MIE.

3.2. Validation of the present approach for the MIE prediction

In this section, the proposed MIE prediction model is validated against the analytical models reported in equations (1) and (2) and a number of experimental data available in the literature concerning the determination of MIE at atmospheric conditions (1 bar, 298 K).

Propane was selected as the first fuel. The reaction mechanism developed by Blanquart et al. [30] was used in the Cantera simulations detailed at the top of Section 3, and the results for S_L^0, T_a and Le are displayed in Figure 4(a). Then, Figure 4(b) presents the MIE values predicted with the present approach compared to the literature analytical models and the experimental outcomes of Lewis and Von Elbe [1] and of Randeberg and Eckhoff [3], the latter being the lowest literature MIE values. For equations (1) and (2), the quenching distance values were set as a multiple of the laminar flame thickness, δ_L, and, in accordance with the relevant experimental investigations, the value $d_q = 6\delta_L$ was chosen [1] [12]. Moreover, for the two literature models, two different methods were used to express δ_L: $\delta_{grad} = (T_{ad} - T_u)/(dT/dx)_{max}$, which uses the maximum temperature gradient of the simulated planar flame, and δ_{FWHM}, representing the full-width at half maximum (FWHM) of the temperature gradient profile [16]. Consequently, two MIEs were calculated for each model, for a total of four values.

The comparison of present model predictions, analytical outcomes, and experimental data for the MIE shows that equations (1) and (2) overestimate it compared to the results from Lewis and Von Elbe, yielding MIE values almost two orders of magnitude higher than those provided by Randeberg and Eckhoff. On the contrary, the present MIE prediction approach based on the present authors' kernel expansion model provides a more consistent and satisfying MIE estimation, with values very close to those reported by Lewis and Von Elbe for a wide range of propane volume concentrations, with $\phi = 1$ corresponding to 4.04%. The lowest MIE is approximately 0.15 mJ at 4.8% concentration ($\phi \cong 1.2$), and it falls between the two sets of experimental data. The discrepancies are very likely due to the different characteristics of the ignition systems, but since the present electrodes are similar to those used by Lewis and Von Elbe, predicting MIE values closer to their outcomes is not surprising. Moreover, since propane has similar properties to those of conventional gasolines [11], the good results obtained here suggest that the present approach could have much wider validity.

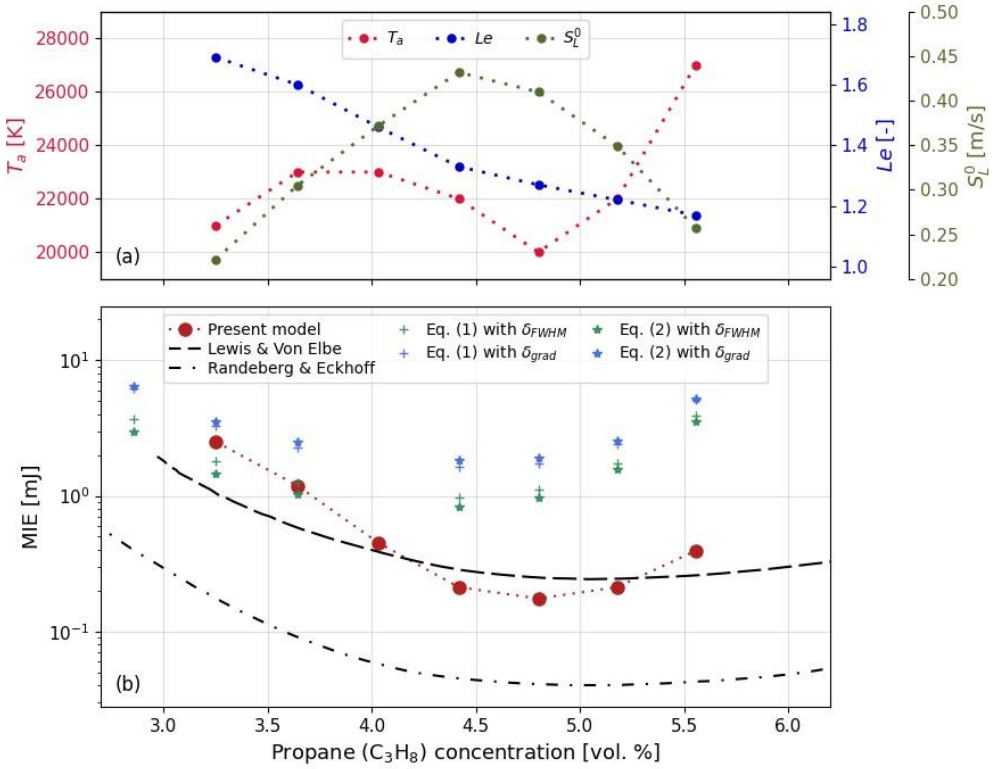

Figure 4 – T_a, Le and S_L^0 (a) and MIE (b) for propane/air mixtures over fuel volume concentration.

The second fuel examined in this work is hydrogen, and the results for the MIE of hydrogen/air mixtures spark-ignited at atmospheric conditions are reported in Figure 5. In the simulations of the planar adiabatic flames, the GRI-Mech 3.0 [31] was used and $d_q = 2.5\delta_L$ was adopted as suggested by Cirrone et al. after calibration with the experimental data [13].

As Figure 5(b) shows, the results obtained using equations (1) and (2) are generally reasonable, but there is a noticeable MIE overestimation near the stoichiometric concentration (29.6% for $\phi = 1$) and for leaner mixtures. Concerning the present MIE predictions, the proposed approach follows well the trend observed by Lewis and Von Elbe in the rich-mixture area, but it tends to yield lower MIE values. Apart from the ignition system differences, it is possible that this discrepancy may simply come from the unsuitability of adjustment coefficients C_A and C_T, validated for propane (and likely to be similarly valid for long-chained hydrocarbon fuels), but not for lighter fuels such as hydrogen. Then, around the stoichiometric concentration, the MIE predictions match much more closely the experimental values, but as the mixture becomes leaner the modelled MIE drops by an order of magnitude. This sudden decrease, inconsistent with the experiments, is caused by the Lewis number dropping below 1. This happens because as $Le < 1$ the flame stretch starts raising the burning temperature, leading to a super-adiabatic kernel that experiences simultaneously a critical radius decrease and an expansion speed increase [20]. This results in the present MIE prediction approach losing its main extinction driver, and the kernel survival can be easily achieved with very low ignition energy. A similar phenomenon, although measurably less pronounced, occurs for methane at $\phi = 0.9$, for which $Le \cong 1$ and the MIE of 0.08 mJ predicted by this model clashes with the value of 0.3 mJ reported by Lewis and Von Elbe.

These outcomes suggest that when $Le \leq 1$ the detrimental effects of flame stretch on the kernel growth act mainly at the very beginning of the expansion, that is when the plasma column tries to expand towards a spherical kernel but fails to do so. However, it seems evident that the simplified modelling strategies elucidated in Section 2.3 are unsuited to replicate this complicated expansion, clearly indicating a possible path for future developments.

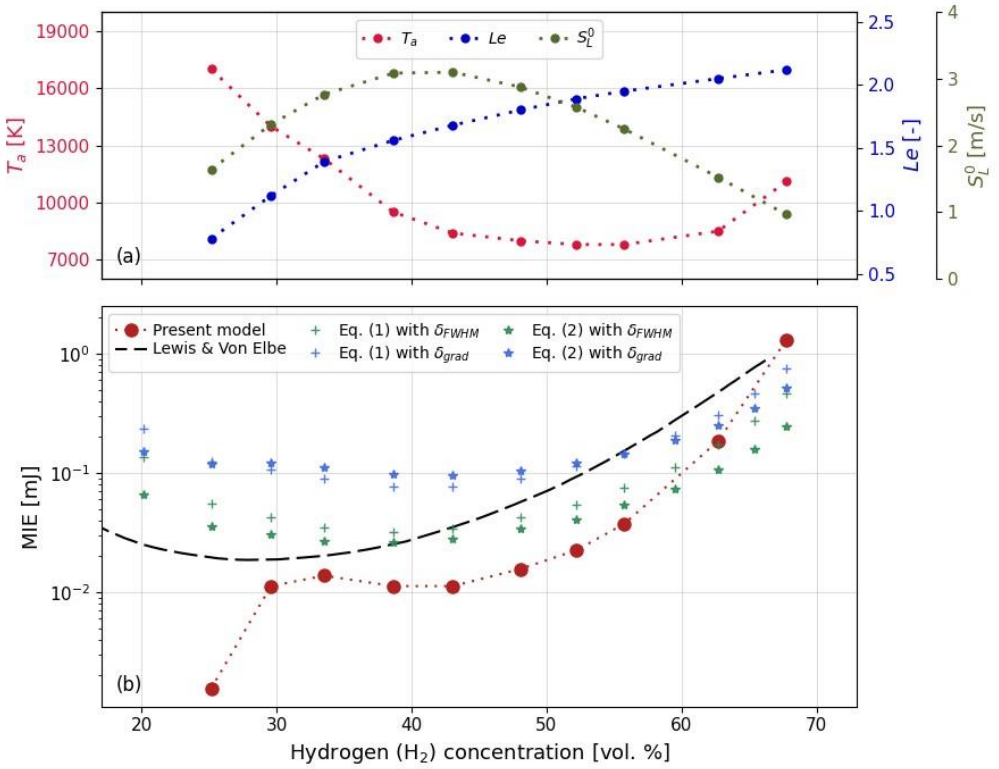

Figure 5 – T_a, Le and S_L^0 (a) and MIE (b) for hydrogen/air mixtures over fuel volume concentration.

3.3. Effect on the MIE of increasing pressure and temperature up to engine-relevant conditions

Finally, for SI engines it is important to quantify the MIE at unburned pressures and temperatures much higher than ambient ones, because these represent the practical engine operating conditions. These two effects are addressed separately in Figure 6, with Figure 6(a) showing the change in MIE of a propane-air mixture with $\phi = 0.8$ at 298 K as the pressure increases from 1 to 20 bar, and Figure 6(b) presenting the same change as a function of temperature at a constant pressure of 1 bar. In these simulations the MIE values are not those for the optimal gap sizes, but they are computed for fixed gap distances, as is the case for SI engine plugs. Three distances were used, 1 mm, 2.5 mm, and 5 mm, with the specific values chosen only to conduct an effective sensitivity analysis of the MIE predictions to this parameter and without aiming to replicate the actual gap sizes encountered in SI engines.

Firstly, Figure 6(a) shows that the MIE decreases with increasing pressure, but it does so very rapidly before stabilizing to approximately constant values. Additionally, at low pressure a larger d_g is more favourable, because if d_g is small the flame kernel is averagely larger and enters into contact with the electrodes immediately after the ignition, hence losing heat much sooner. However, as the ignition energy decreases, the kernel size also decreases, and smaller d_g minimize the detrimental effects caused by the elongation of the plasma column. Secondly, regarding Figure 6(b) the analysis is more straightforward, because increasing T_u always leads to smaller MIE values, as expected since S_L^0 rises quickly with T_u but Le does not [11]. Then, a similar trend as before is observed concerning d_g and the quenching effect of the electrodes.

All these results are fully consistent with the typical use of small plug gaps (1 mm or below) in conventional SI engines, but they also suggest that under very specific circumstances, such as the reduced pressure and temperature conditions experienced by the unburned mixture at low engine loads, larger gaps could actually provide beneficial effects.

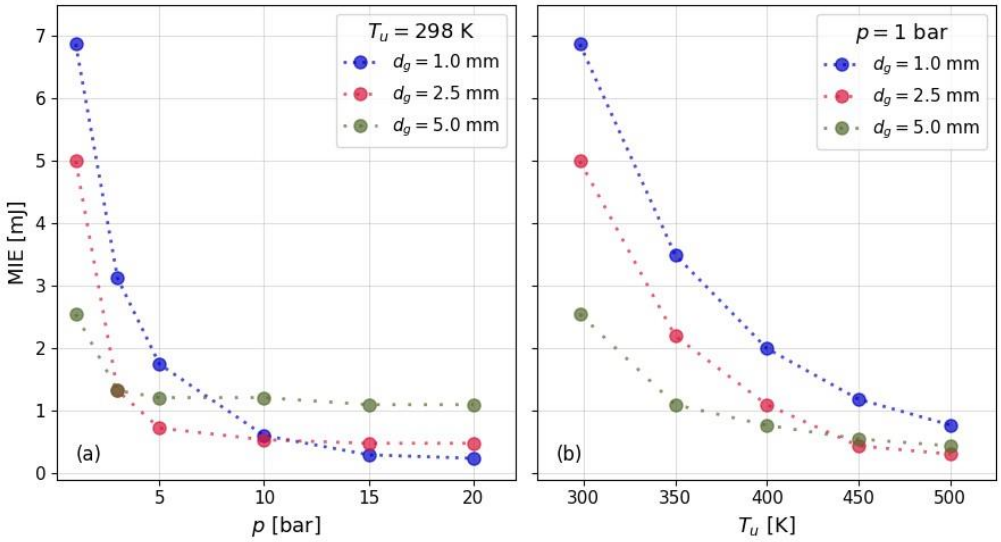

Figure 6 – MIE for $\phi = 0.8$ propane/air mixture at different pressures (a) and temperatures (b).

4. Conclusions and future developments

Estimating the MIE of spark-ignited fuel/air mixtures is an important aspect for proper prediction of SI engine performance, but the many experiments conducted cannot be explained by analytical prediction models, whereas numerical methods are more accurate but also very time-consuming. In this work, the MIE estimation has been conducted with a novel modelling approach, which is based on the application of a modified version of a novel analytical flame kernel expansion model proposed by the authors. This model is based on the conservation equations for mass, species, and energy of the spherical kernel, supported by elements of the thermodiffusive theory for estimating the reactant and temperature gradients at the flame front, while its initial conditions come from the solution of cylindrical conservation equations applied to the plasma volume that expands due to the shock wave caused by the electrical breakdown. The model, able to capture the kernel extinction due to flame stretch, accounts for different fuels and equivalence ratios through key parameters such as laminar flame speed, Lewis number, and activation temperature of the one-step global combustion reaction.

Proper estimation of the MIE is made very complex by the difficult quantification of the impact of the electrodes on the flame kernel development, and analysis of literature experimental data indicates that this impact mainly consists in *i)* the heat losses towards the electrodes (quenching), and *ii)* the elongation of the plasma column formed by the breakdown process. Preliminary modelling steps have been made in this work to account for these elements, in particular by adding a heat loss term to quantify the contribution of the electrodes to the kernel quenching and by introducing an 'effective' kernel radius that accounts for the cylinder-to-sphere transition, stronger at larger gap distances d_g.

Concerning the results, the MIE-d_g relationship appears quite consistent with literature evidence, and the comparison of the present MIE predictions with both analytical models and experimental data on the MIE of propane/air mixtures at atmospheric conditions is good across all equivalence ratios. On the other hand, for stoichiometric and rich hydrogen/air mixtures the predicted MIE is lower than the experimental evidence, and for lean mixtures the underestimation becomes very high, reaching about one order of magnitude. The cause seems related to a not fully adequate modelling of the impact of the electrodes on the flame kernel at the beginning of the expansion, which is particularly evident at the Lewis numbers $Le \leq 1$ that characterize lean hydrogen/air mixtures. Finally, the approach was tested at fixed gap size up to engine-relevant unburned mixture conditions, showing satisfactory trends.

The present work has shown that the novel model introduced by the authors to predict the flame kernel development after spark ignition coupled with the modifications introduced to estimate the MIE

by accounting for spark-plug-related effects is trending in the right direction, especially in the case of propane. This is a key aspect, because propane behaves very similarly not only to the gasolines and gasoline-like fuels used in conventional SI engines, but also to the carbon-neutral e-fuels touted as key components of the future power generation. However, and particularly at low Lewis numbers, the approach still requires some improvements, especially in determining the property-related adjustment coefficients of the expansion model, in modelling the effect of the plasma column elongation, possibly with a more theoretically consistent approach, and in accounting for the electrode quenching effects.

Acknowledgements
The work was supported by the co-financing of the European Union - FSE-REACT-EU, PON Research and Innovation 2014-2020 DM 1062/2021. The financial support of the DPIA of the University of Udine under the strategic program “PSD-ESPERT” is also gratefully acknowledged.

References

[1] B. Lewis and G. Von Elbe, Combustion, Flames, and Explosion of Gases, 3rd edition, New York: Academic Press, 1987.

[2] J. Moorhouse, A. Williams and T. Maddison, "An investigation of the minimum ignition energies of some C1 to C7 hydrocarbons," *Combustion and Flame,* vol. 23, no. 2, pp. 203-213, 1974.

[3] E. Randeberg and R. K. Eckhoff, "Measurement of minimum ignition energies of dust clouds in the <1 mJ region," *Journal of Hazardous Materials,* vol. 140, no. 1-2, pp. 237-244, 2007.

[4] R. K. Eckhoff, M. Ngo and W. Olsen, “On the minimum ignition energy (MIE) for propane/air,” *Journal of Hazardous Materials,* vol. 175, no. 1-3, pp. 293-297, 2010.

[5] S. P. M. Bane, J. E. Shepherd, E. Kwon and A. C. Day, “Statistical analysis of electrostatic spark ignition of lean H2/O2/Ar mixtures,” *International Journal of Hydrogen Energy,* vol. 36, no. 3, pp. 2344-2350, 2011.

[6] A. Wähner, G. L. T. Gramse and M. Beyer, "Determination of the minimum ignition energy on the basis of a statistical approach.," *Journal of Loss Prevention in the Process Industries,* vol. 26, no. 6, pp. 1655-1660, 2013.

[7] C. Wu, R. Schießl and U. Maas, "Numerical studies on minimum ignition energies in methane/air and iso-octane/air mixtures," *Journal of Loss Prevention in the Process Industries,* vol. 72, p. 104557, 2021.

[8] H. Lu, F. Liu, K. Wang and al., “Numerical study on the minimum ignition energy of a methane-air mixture,” *Fuel,* vol. 285, p. 119230, 2021.

[9] M. Pretto, P. Giannattasio, E. De Betta and F. Bozza, “A consistent model of the initiation, early expansion, and possible extinction of a spark-ignited flame kernel,” *International Journal of Engine Research,* 2024, online at: http://doi.org/10.1177/14680874241272812.

[10] M. Champion, B. Deshaies and G. Joulin, “Relative influences of convective and diffusive transports during spherical flame initiation,” *Combustion and Flame,* vol. 74, no. 2, pp. 161-170, 1988.

[11] S. R. Turns, An Introduction to Combustion: Concepts and Applications, 2nd edition, New York, NY, USA: McGrawHill Companies, 2000.

[12] C. Movileanu, M. Mitu, V. Giurcan and al., “Quenching distances, minimum ignition energies and related properties of propane-air-diluent mixtures,” *Fuel,* vol. 274, p. 117836, 2020.

[13] D. Cirrone, D. Makarov, C. Proust and V. Molkov, "Minimum ignition energy of hydrogen-air mixtures at ambient and cryogenic temperatures," *International Journal of Hydrogen Energy,* vol. 48, no. 43, pp. 16530-16544, 2023.

[14] L. He, "Critical conditions for spherical flame initiation in mixtures with high Lewis numbers,"

Combustion Theory and Modelling, vol. 4, no. 2, pp. 159-172, 2000.

[15] A. P. Kelley and C. K. Law, "Nonlinear effects in the extraction of laminar flame speeds from expanding spherical flames," *Combustion and Flame,* vol. 156, no. 9, pp. 1844-1851, 2009.

[16] C. J. Sun, C. J. Sung, L. He. and C. Law, "Dynamics of Weakly Stretched Flames: Quantitative Description and Extraction of Global Flame Parameters," *Combustion and Flame,* vol. 118, no. 1-2, pp. 108-128, 1999.

[17] A. P. Kelley, G. Jomaas and C. K. Law, "Critical radius for sustained propagation of spark-ignited spherical flames," *Combustion and Flame,* vol. 156, no. 5, pp. 1006-1013, 2009.

[18] G. Meyer and A. Wimmer, "A thermodynamic model for the plasma kernel volume and temperature resulting from spark discharge at high pressures," *Journal of Thermal Analysis and Calorimetry,* vol. 133, no. 2, pp. 1195-1205, 2018.

[19] P. Giannattasio, M. Pretto and E. De Betta, "A phenomenological model for predicting the early development of the flame kernel in spark-ignition engines," *Journal of Physics: Conference Series,* vol. 2648, no. 1, p. 012070, 2023.

[20] D. Yu and Z. Chen, "Theoretical analysis on the transient ignition of a premixed expanding flame in a quiescent mixture," *Journal of Fluid Mechanics,* vol. 924, p. A22, 2021.

[21] Y. Ko, V. S. Arpaci and R. W. Anderson, "Spark ignition of propane-air mixtures near the minimum ignition energy: Part II. A model development," *Combustion and Flame,* vol. 83, no. 1-2, pp. 88-105, 1991.

[22] T. Langer, G. Gramse, D. Möckel and al., "MIE experiments and simultaneous measurement of the transferred charge–A verification of the ignition threshold limits," *Journal of Electrostatics,* vol. 70, no. 1, pp. 97-104, 2012.

[23] S. Stepanyan, N. Minesi, A. Tibère-Inglesse and al., "Spatial evolution of the plasma kernel produced by nanosecond discharges in air," *Journal of Physics D: Applied Physics,* vol. 52, no. 29, p. 295203, 2019.

[24] O. Ekici, O. A. Ezekoye, M. J. Hall and R. D. Matthews, "Thermal and flow fields modeling of fast spark discharges in air," *Journal of Fluids Engineering,* vol. 129, no. 1, pp. 55-65, 2007.

[25] O. Colin, M. Ritter, C. Lacour, K. Truffin, S. Mouriaux, S. Stepanyan, B. Lecordier and P. Vervisch, "DNS and LES of spark ignition with an automotive coil," *Proceedings of the Combustion Institute,* vol. 37, no. 4, pp. 4875-4883, 2019.

[26] S. Essmann, D. Markus, H. Grosshans and U. Maas, "Experimental investigation of the stochastic early flame propagation after ignition by a low-energy electrical discharge," *Combustion and Flame,* vol. 211, pp. 44-53, 2020.

[27] D. G. Goodwin, H. K. Moffat, I. Schoegl and al., "Cantera: An Object-oriented Software Toolkit for Chemical Kinetics, Thermodynamics, and Transport Processes," Version 2.5, 2021. [Online]. Available: https://www.cantera.org. [Accessed 6 May 2024].

[28] J. K. Bechtold and M. Matalon, "The dependence of the Markstein length on stoichiometry," *Combustion and Flame,* vol. 127, no. 1-2, pp. 1906-1913, 2001.

[29] R. Addabbo, J. K. Bechtold and M. Matalon, "Wrinkling of spherically expanding flames," *Proceedings of the Combustion Institute,* vol. 29, no. 2, pp. 1527-1535, 2002.

[30] G. Blanquart, P. Pepiot-Desjardins and H. Pitsch, "Chemical mechanism for high temperature combustion of engine relevant fuels with emphasis on soot precursors," *Combustion and Flame,* vol. 156, no. 3, pp. 588-607, 2009.

[31] G. P. Smith, D. M. Golden, M. Frenklach and al., "GRI Mech 3.0," [Online]. Available: http://www.me.berkeley.edu/gri_mech/. [Accessed 2 May 2024].